



OPEN ACCESS

EDITED BY

Tao Zhang,
University of Science and Technology
Beijing, China

REVIEWED BY

Jiaxing Chen,
University of Shanghai for Science and
Technology, China
Xu Song,
Ludong University, China

*CORRESPONDENCE

Li Tianzhi,
✉ ltzneo@qq.com

RECEIVED 09 March 2023

ACCEPTED 21 April 2023

PUBLISHED 09 May 2023

CITATION

Haoting Q, Tianzhi L, Jianhua L, Yunxia W
and Hongtao S (2023), Optimal operation
of cascaded hydropower plants in hydro-
solar complementary systems
considering the risk of unit vibration
zone crossing.
Front. Energy Res. 11:1182614.
doi: 10.3389/fenrg.2023.1182614

COPYRIGHT

© 2023 Haoting, Tianzhi, Jianhua, Yunxia
and Hongtao. This is an open-access
article distributed under the terms of the
[Creative Commons Attribution License
\(CC BY\)](https://creativecommons.org/licenses/by/4.0/). The use, distribution or
reproduction in other forums is
permitted, provided the original author(s)
and the copyright owner(s) are credited
and that the original publication in this
journal is cited, in accordance with
accepted academic practice. No use,
distribution or reproduction is permitted
which does not comply with these terms.

Optimal operation of cascaded hydropower plants in hydro-solar complementary systems considering the risk of unit vibration zone crossing

Qin Haoting¹, Li Tianzhi^{1*}, Li Jianhua^{1,2}, Wu Yunxia¹ and Song Hongtao³

¹Southwest Electric Power Design Institute Co., Ltd. of China Power Engineering Consulting Group, Chengdu, China, ²School of Electrical Engineering, Sichuan University, Chengdu, China, ³School of Electrical Engineering and Information, Southwest Petroleum University, Chengdu, China

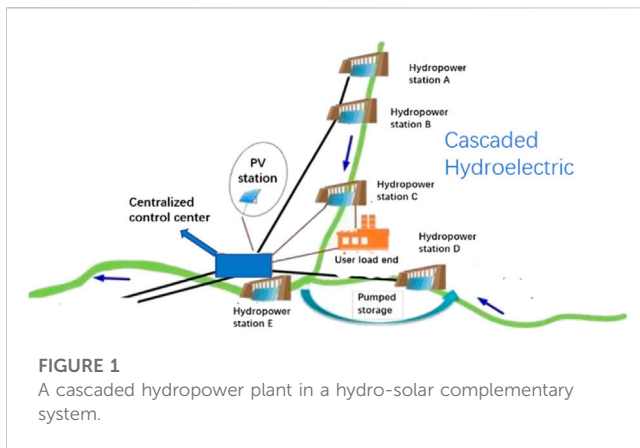
With the undergoing adjustment of the national energy structure of China, developing cascaded hydropower plants in hydro-solar complementary systems becomes an important way to optimize the energy structure. This study focuses on the risk that solar energy disturbances induce large load transfers between hydropower units that can cause hydropower units to frequently cross their vibration zones. Vibration zone crossing can further cause wear of mechanical components of hydropower units. To this end, considering the requirement of avoiding vibration zone crossing, the concept of the vibration zone crossing risk coefficient is introduced and a cascaded hydropower plant optimal operation model considering the risk of vibration zone crossing is proposed. Moreover, this is two-layer algorithm. This layer of algorithms includes improved migration model and migration operator is proposed to solve this mean a cascaded hydropower plant optimal operation model considering the risk of vibration zone crossing. Numerical simulation results based on the data of an actual hydropower plant are used to validate the proposed model and (IBBO-DP) algorithm.

KEYWORDS

hydropower, vibration zone crossing, hydro-solar complementary systems, biogeography-based optimization, load distribution

1 Introduction

With the adoption of carbon peaking and carbon neutrality goals and under the development direction of building emerging power systems, clean energy such as hydropower and photovoltaics (PV) present an opportunity for rapid development. Considering the variability and uncertainty of solar energy which is strongly related to the climate and environment, large-scale direct integration could pose threats to a hydro-solar complementary system operational security and stability. As shown in [Figure 1](#), in a hydro-solar complementary system, cascaded hydropower plants can leverage the regulation ability of their reservoirs to mitigate the fluctuation, uncertainty, and intermittency of solar energy, thereby improving the overall power generation and peak-shaving capacity of the hydro-solar complementary system. However, for a cascaded hydropower plant that responds to the fluctuations in solar energy, its power output adjustments could increase significantly and the resulting frequent adjustments of the governor would lead to the frequent



startup of the oil pressure pump, large water level changes of the turbine cover, and a high operating temperature of the bearing bush. Moreover, simply adopting the traditional load distribution and unit commitment strategy of cascaded hydropower plants will not only cause large-scale load transfers between the units in a short period but also lead to hydropower units frequently crossing their vibration zones, which might shorten the service life of water guide mechanisms and rotating parts of the units and might even cause damages. This should be avoided as much as possible in the actual production scenario.

In recent years, many researchers have focused on the optimal dispatch of cascaded hydropower plants in the hydro-solar complementary system. Existing works mainly focus on the aspects of operational characteristics (Zhu et al., 2021; Ye et al., 2018), complementary generation mechanism (An et al., 2015; Yu et al., 2020), optimal unit capacity configuration (Bai et al., 2018; Li et al., 2018; Zhao et al., 2018), and the interaction analysis of solar energy and hydropower (Zhu et al., 2020). Focusing on resolving the problem of the unit frequently crossing the vibration zones during the load distribution process, a lot of research has been carried out from the perspective of optimal load distribution (Zhang et al., 2019; Xu et al., 2022) and accurate formulation of vibration zones (Yang et al., 2019; Zhi et al., 2019). Considering multiple complex constraints such as multi-vibration areas and power adjustment ranges, Hu et al. (2017) determined the feasible adjustment domain of different unit commitments by dividing the operating interval and using the interval combination theory to limit the number of times that the units enter their vibration areas. Yang et al. (2019) adopted a merit order of power generation efficiency of the units to determine their operating ranges and then optimized the load distribution. Cheng et al. (2016) and Zhao et al. (2021) modeled the irregular vibration zones with linear constraints and cast the load distribution problem as a mixed integer linear programming problem.

The biogeography-based optimization (BBO) algorithm has been widely used in the optimal scheduling of multi-energy complementary systems (Ren et al., 2023; Jiang et al., 2018) and fast response decision-making of the systems (Sun et al., 2013; Zhao et al., 2013) due to its strong convergence ability and compatibility. Gong et al. (2011) and Tian et al. (2018) applied the BBO algorithm in an optimal operation of the wind-hydro complementary system with improvements in migration models and mutation operators.

However, the aforementioned works have seldom considered the risk of hydropower units crossing their vibration zones in an

actual operation. Moreover, to jointly optimize load distribution and unit commitment, usually, traditional solving methods such as the ordinal priority approach and linear programming are adopted. However, these methods may fail to provide solutions with acceptable accuracy and optimality within a limited time, especially when facing multiple restrictions in the actual operation, such as avoiding the vibration and cavitation zones and dealing with complicated multi-unit and multi-vibration situations. Consequently, the efficiency and accuracy requirements of unit operation scheduling cannot be fully satisfied.

To better guarantee operational safety while pursuing economic benefits in the optimal operation, on the basis of existing works, this study focuses on the problem of optimally distributing the load among the units within a cascaded hydro-power plant under the background of a hydro-solar complementary system. Considering the inevitable “reversal effect” of cascaded hydropower plants and the low moment of inertia characteristic of PVs, PV power output fluctuations can easily induce low-frequency oscillations and other risks. To this end, considering the requirement of avoiding the hydropower unit’s vibration zones, the unit vibration zone crossing risk factor is introduced and based on it, a cascaded hydroelectric unit optimal operation model with constraints such as vibration zone constraints, unit startup constraints, and unit output fluctuation constraints is proposed. The proposed model can greatly reduce the risk of hydropower units crossing their vibration zones and improve the operational stability of cascaded hydropower plants. Moreover, focusing on the proposed model, by combining the BBO algorithm with the dynamic programming (DP) algorithm, an improved biogeography-based optimization–dynamic programming (IBBO-DP) two-layer algorithm is proposed. In which, the outer layer that consists of DP determines the unit commitment, and the inner layer that consists of BBO optimizes the load distribution between the units. By improving the migration model and mutation operators in the BBO algorithm, the convergence ability and solution optimality are enhanced. When compared with the traditional algorithms, in the load distribution problem, the proposed algorithm achieves a 10.6% saving on water usage and reduces the vibration zone crossing by 24 times in the case study.

The contributions of this article are twofold:

The concept of the vibration zone crossing risk coefficient is introduced and on this basis, a cascaded hydropower plant optimal operation model considering the risk of vibration zone crossing is proposed.

An algorithm that combines the BBO algorithm and DP with enhanced convergence ability and solution optimality is proposed to solve the cascaded hydropower plant optimal operation model.

2 Cascaded hydropower optimal operation model considering the risk of vibration zone crossing

2.1 Objective of optimal operation model

For a cascaded hydropower plant in a hydro-solar complementary system, the load distribution among its units and unit commitment should consider safe operation requirements, such as avoiding vibration areas, unit inflow rates, unit startup and

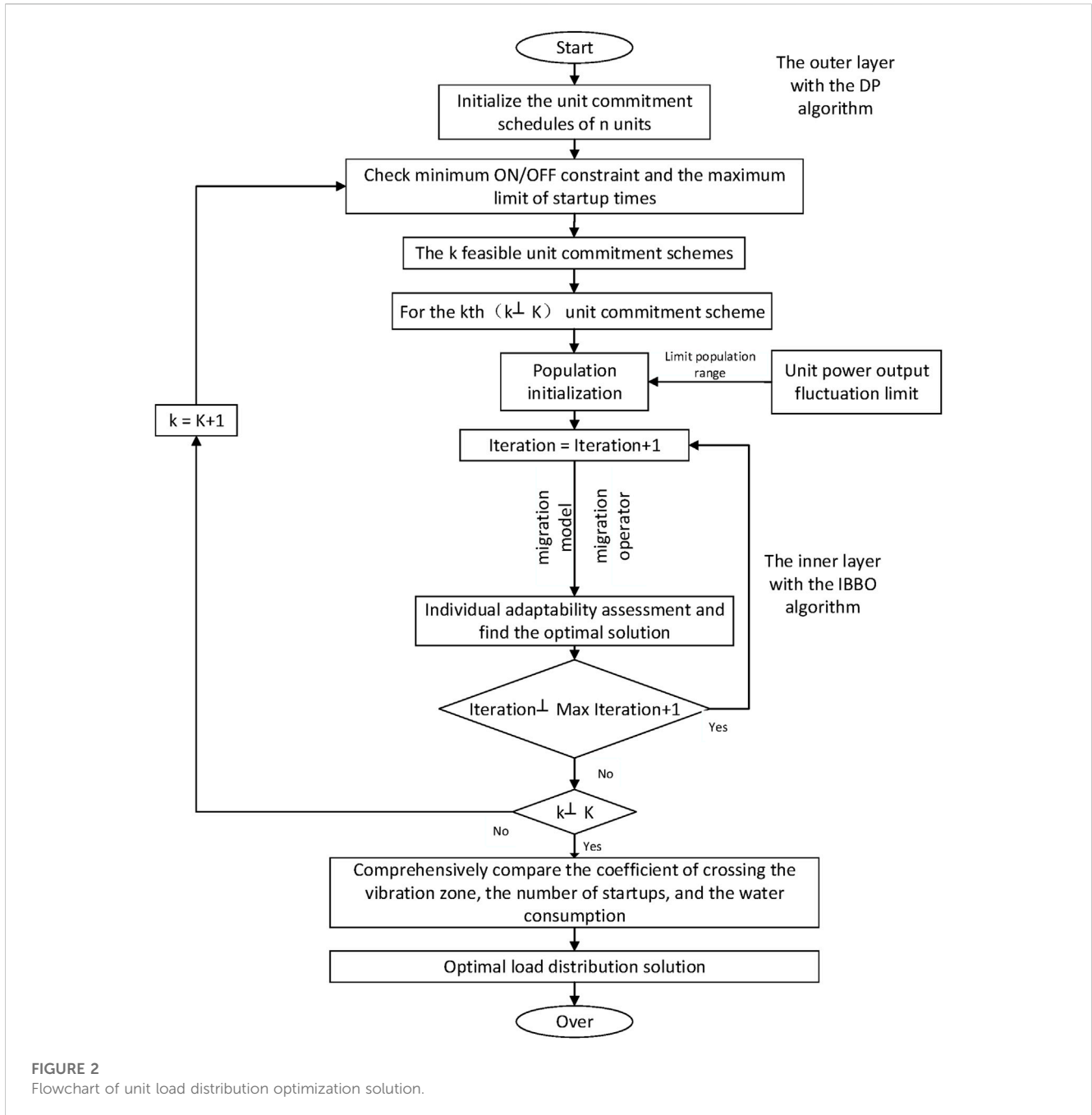


FIGURE 2
Flowchart of unit load distribution optimization solution.

shutdown times in different periods, and unit minimum ON/OFF time limits, as well as economical requirements, while satisfying the step load curve. The objective of the cascaded hydropower plant is to minimize the unit water usage as in Eq. 1, where I is the number of units in the plant and T represents the number of time intervals within the scheduling time horizon. $Q(H_t, P_{i,t})$ is the power-to-water conversion function that calculates the water usage corresponding to the power output $P_{i,t}$ under a certain water head H_t at a time interval t . Δt indicates the timespan of the time intervals. The binary variable $\lambda_{i,t}$ represents the ON/OFF status of the unit i at the time interval t . W_{on} is the equivalent water usage of conducting startup. $n_{i,cross}$ is number of times that unit i crosses its vibration zone. W_{cross} is the equivalent water usage

of the crossing vibration zones. Particularly, this study introduces the vibration zone crossing risk coefficient to quantify the risk of a unit crossing its vibration zones.

$$W = \min \sum_{i=1}^I \sum_{t=1}^T \left(Q(H_t, P_{i,t}) \times \Delta t + \lambda_{i,t} (1 - \lambda_{i,t-1}) \times W_{on} + n_{i,cross} \times W_{cross} \right). \quad (1)$$

2.2 Constraints of optimal operation model

The constraints of the proposed cascaded hydropower optimal operation model include the output upper and lower bounds of the

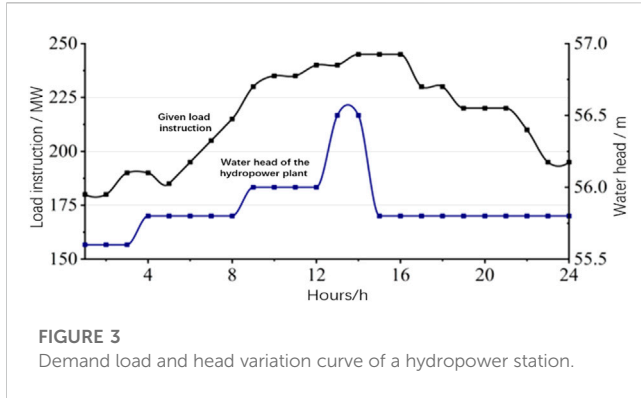


FIGURE 3 Demand load and head variation curve of a hydropower station.

units, load balance constraint, and reservoir outflow limits (Feng et al., 2012). Moreover, in determining the unit commitment, constraints such as unit vibration zones, unit minimum ON/OFF time, and the number of startup times are enforced. A part of the abovementioned constraints is detailed below.

The vibration zone constraint is formulated as in Eq. 2, where $P_{i,t}$ represents the power output of unit i in time interval t . \bar{P}_i and P_i are the upper and lower bounds of its vibration zone.

$$(P_{i,t} - \bar{P}_i)(P_{i,t} - P_i) \geq 0. \tag{2}$$

The unit minimum ON/OFF time is limited by constraint (3), where T_i^{on} and T_i^{off} represent the continuous ON and OFF times of unit i , respectively. $T_{i,min}^{on}$ and $T_{i,min}^{off}$ are the minimum ON and OFF times of unit i , respectively.

$$(T_i^{on} - T_{i,min}^{on})(T_i^{off} - T_{i,min}^{off}) \geq 0. \tag{3}$$

The number of startup times is limited by constraint (Eq. 4). In Eq. 4, $N_{i,t}^{on}$ represents the startup at time t of unit i . N_{max}^{on} represents the allowed maximum number of startup times.

$$0 \leq \sum_{t=1}^T \sum_{i=1}^I N_{i,t}^{on} \leq N_{max}^{on}. \tag{4}$$

To avoid the situation where units cross their vibration zones or dramatically adjust their power outputs when the load fluctuates greatly in a period, the unit power output fluctuation limit is added to the model. If a unit is started up at the time interval t , to reduce the power output fluctuation of other ON units, the power output of the newly started up unit is required to satisfy constraint (Eq. 5). In Eq. 5, $P_{i,t}^n$ represents its power output; $P_{i,min}^n$ and $P_{i,max}^n$ represent the upper and lower bounds of its feasible zone n , respectively.

$$P_{i,min}^n \leq P_{i,t}^n \leq P_{i,max}^n. \tag{5}$$

We use $Z_{1,t}$, $Z_{2,t}$, ..., $Z_{n,t}$ to indicate the unit commitment at time interval t , and use Z_{t-1} to indicate the optimal unit commitment at time interval $(t - 1)$. For time interval t , using the total output power of the newly started-up units, the total power transfer of the shutdown units, and the load change in time interval t , the allowed range of power output variation of the remaining ON units can be determined and enforced as in Eqs 6, 7. $\sum_{i=1}^{I1} P_{i,t}^*$ represents the total power output of $I1$ newly started up

units in time interval t . If no unit is committed, this term equals to 0. $\sum_{i=1}^{I2} P_{i,t}^*$ represents the total power output transfer due to shutdown of $I2$ units from time interval $t - 1$ to t . If no unit is uncommitted, this term equals 0. $\sum_{i=1}^I P_{i,t-1} - P_t$ represents the load fluctuation, which equals the difference between the total power output of time interval $(t - 1)$ minus the load of time interval t . $P_{i,t}^{on}$ represents the output of unit i continuously operating in time period t .

$$\Delta P = \sum_{i=1}^{I1} P_{i,t}^* - \sum_{i=1}^{I2} P_{i,t-1}^* - \left(\sum_{i=1}^I P_{i,t-1} - P_t \right), \tag{6}$$

$$\max \left(\sum_{i=1}^{I_{on}} P_{i,t-1}^{on} - \Delta P, P_{i,min}^n \right) \leq P_{i,t}^{on} \leq \min \left(\sum_{i=1}^{I_{on}} P_{i,t-1}^{on} + \Delta P, P_{i,max}^n \right). \tag{7}$$

When the units without commitment change in time interval t is the majority, to further limit the output change ΔP , ΔP is updated according to Eq. 8.

$$\begin{cases} \Delta P = \Delta P - \sum_{i=1}^{I_{on}} (P_{i,t}^{on} - P_{i,t-1}^{on}), \sum_{i=1}^I P_{i,t-1} < P_t \\ \Delta P = \Delta P - \sum_{i=1}^{I_{on}} (P_{i,t}^{on} - P_{i,t-1}^{on}), \sum_{i=1}^I P_{i,t-1} > P_t \end{cases}. \tag{8}$$

If no unit is committed or uncommitted in time interval t , that is, unit commitment does not change, the load fluctuation is evenly distributed to all ON units as in Eq. 9. In Eq. 9, n_{on} is the continuous ON units between two consecutive time intervals.

$$\Delta P = \frac{\sum_{i=1}^I P_{i,t-1} - P_t}{n_{on}}. \tag{9}$$

3 Improved biogeography-based optimization algorithm

3.1 Traditional biogeography-based optimization algorithm

The core idea of the traditional biogeography algorithm (Chen et al., 2012) is to simulate the migration and emigration of adjacent individuals in the process of evolution combining the mutation of individuals in exploring the optimal solution. The problem of load distribution and unit commitment in cascaded hydropower plants is a large-scale non-linear optimization problem. The traditional biogeography algorithm with an overly simplified species migration curve can hardly simulate the biological migration with high accuracy, which makes it unable to adapt to the complex load distribution problem of hydropower plants.

3.2 Based on IBBO-DP double nesting algorithm

To this end, this study proposes an IBBO-DP two-layer algorithm that combines a biogeography-based optimization algorithm and a dynamic programming algorithm and improves the migration model and migration operator to solve

TABLE 1 Comparisons of the four algorithms.

Algorithm	A (IBBO-DP)	B (IBBO)	C (BBO)	D (DDP)
Total water usage (10^7 m^3)	3.9708	4.0235	4.0318	4.2548
Total water usage rate ($10^4 \text{ m}^3/\text{s}$)	4.4119	4.4716	4.4786	4.5148
Water consumption rate (%)	76.50	77.22	77.33	78.45
Startup times	0			
Vibration zone crossing times	0			20

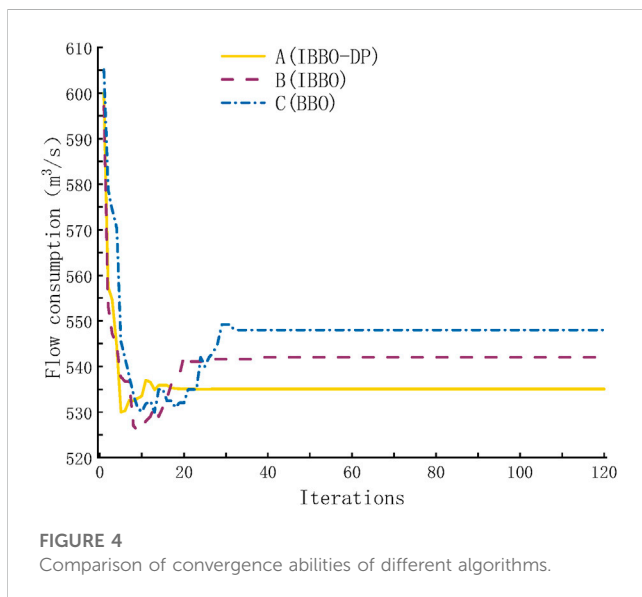


FIGURE 4 Comparison of convergence abilities of different algorithms.

the cascaded hydropower optimal operation model. While considering the constraints of the unit commitment problem, such as vibration zone crossing constraints and minimum ON/OFF time constraints, the unit power output change constraints are enforced. Based on the optimal power output in the previous time interval, this could avoid large power output changes of the units when faced with load fluctuations and unit commitment changes. In addition, by leveraging the improved migration model and migration operator (Dong et al., 2014), the load distribution can be optimized. The improved BBO algorithm (Jiang et al., 2018) is embedded into the DP algorithm forming a two-layer intelligent optimization algorithm with the two layers focusing on unit commitment and load distribution, respectively. The outer layer is the DP algorithm, which evaluates the unit commitment schemes and provides a set of feasible unit commitment schemes to the inner layer that is constituted by the BBO algorithm. The inner layer further carries out the load distribution problem to determine the final solution. The two-layer intelligent optimization algorithm can speed up the solving process when compared with the traditional BBO algorithm. The specific steps of the proposed algorithm are as follows:

(1) Preliminary screening with the outer layer: unit commitment schedules are screened with respect to the constraints. For n

hydropower units, there are 2^n unit commitment schemes. At the beginning of each time interval, the 2^n unit commitment schemes are first screened with the minimum ON/OFF constraint and maximum limit of startup times. All unit commitment schemes violating the two types of constraints are excluded. The remaining unit commitment schemes are then stored in the set of feasible unit commitment solutions and passed to the inner layer.

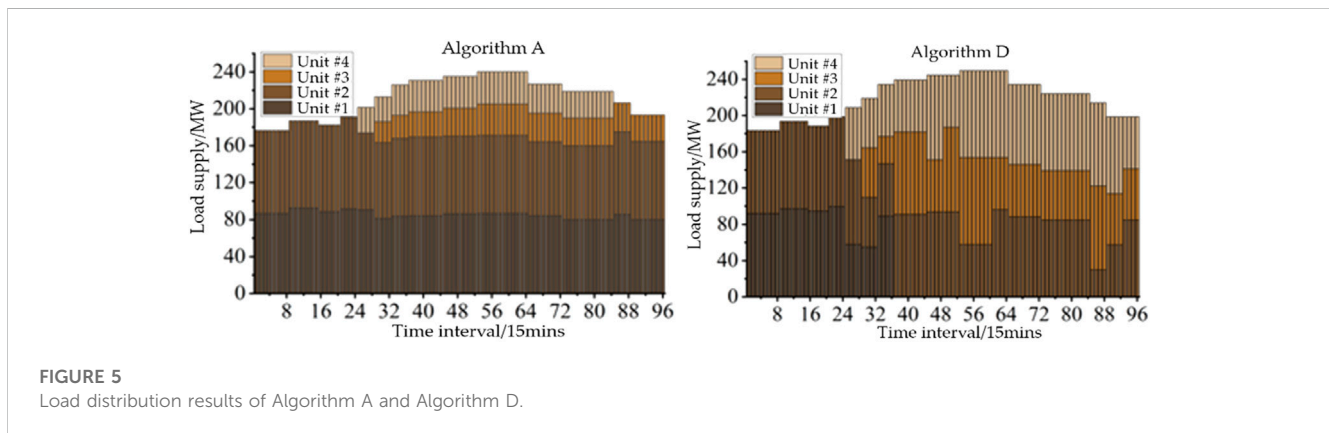
- (2) Load distribution with the inner layer. Load distribution is conducted with each unit commitment scheme in the set. First, the population is initialized. In order to limit the power output changes of hydropower units caused by load fluctuations, in the population initialization stage, initial solutions are generated within a reduced region. The habitability of individual habitats is evaluated. Thereafter, migration models and migration operators are used to perform migration and information cross-exchange on individuals. This expands the search range of the solution. Then, the habitats are sorted after information exchange with respect to their habitability. The unit commitment scheme with the maximum fitness is considered the best solution under the current iteration.
- (3) Optimal solution selection. After a certain number of iterations, the optimal output solution of all unit commitment schemes in the set for time interval t can be obtained. It is necessary to jointly consider the economy and safety in the load distribution problem. The optimal solution to time interval t is selected based on the objective, which comprehensively considers the vibration region crossing coefficients, unit startup times, and water usage.
- (4) Record the load distribution result of the unit commitment scheme for time interval t . If $t \geq 96$, go to step (5); otherwise, return to step (1).
- (5) Record the inflows to the units and calculate the total water usage in the scheduling time horizon. Thereafter, the algorithm terminates.

As the scheduling time horizon is 1 day and the time scale is 15 min, $T = 96$. The flowchart of the proposed solving algorithm is shown in Figure 2.

In Figure 2, N and K denote the number of combinations that meet the constraints after the initial and DP model screening, respectively; k denotes the combination number under the number of K combinations; iteration and max iteration denote the current number of iterations and the preset maximum number of iterations of the improved biography-based optimization algorithm, respectively.

TABLE 2 Output fluctuation index comparison of Algorithms A and D.

Indicator	Unit #1 (%)		Unit #2 (%)		Unit #3 (%)		Unit #4 (%)		Average/%	
	A	D	A	D	A	D	A	D	A	D
S_{AVR}^i	0.6676	5.6932	0.7917	5.9405	0.6475	3.3542	1.0795	2.5325	0.7991	4.3801
S_p^i	0.2388	0.2310	0.9770	0.1499	-0.5207	-0.0253	-0.4758	-0.0736	—	—
S_{ϵ}^i	3.63	5.97	5.12	6.87	3.83	5.33	4.67	8.06	4.31	6.56



4 Case study

4.1 Case settings

In order to validate the rationality and effectiveness of the proposed model and algorithm, the actual operation data of a hydropower plant in China is used to conduct the numerical simulation. This power plant is equipped with four identical 100 MW units. Each unit has three vibration zones distributed between 20 and 100 MW as [20, 35]MW, [55, 60]MW, and [80, 100]MW. The rated water head of the units is 53.4 m. The equivalent water usage of startup/shutdown and the equivalent water usage of vibration zone crossing are $5 \times 10^4 \text{ m}^3/(\text{unit-time})$ and $1 \times 10^5 \text{ m}^3/(\text{unit-time})$, respectively. The scheduling time horizon is a whole day, and the time granularity is set as 15 min, that is, Δt is equal to 15 min. The minimum ON and OFF time are set as 9 h and 1 h, respectively. The load fluctuation range is 5% of the base load, and the load deviation from the system operator’s instructed value is 2%. Figure 3 shows the hourly load curve and the water head curve after 24 h.

4.2 Result analysis

The proposed two-layer intelligent optimization algorithm is compared with the improved BBO (IBBO) algorithm proposed by Jiang et al. (2018), the traditional BBO algorithm, and the two-layer dynamic programming algorithm (DDP) (Zhao et al., 2022). They are indexed as algorithms A, B, C, and D, respectively. Each of the four algorithms solves the cascaded hydropower optimal operation model 50 times. The proposed algorithm and the other compared

algorithms are all implemented in MATLAB. The average results are shown in Table 1.

From Table 1, with the objective of minimizing the total water usage, Algorithm A achieves a lower total water usage than the other three algorithms. The saving is approximately $2.84 \times 10^6 \text{ m}^3$. Moreover, Algorithm A effectively reduces 20 times of vibration zone crossing to 0, which significantly improves operational safety and stability. In fact, Algorithm A shows the best comprehensive performance and outperforms the other three algorithms in total water usage, total water usage rate, and water consumption rate. It can well-balance the safety and economic operation, and provide a more economic operation schedule for hydropower units.

The convergence abilities of Algorithms A, B, and C are compared in Figure 4. It can be seen that Algorithm A converges in approximately 20 iterations and has the fastest convergence speed among the three algorithms. In addition, Algorithm A converges steadily unlike Algorithms B and C which experience an oscillating process when approaching convergence. This verifies that the proposed two-layer intelligent optimization algorithm can speed up the solving process when compared with the IBBO and traditional BBO algorithms.

in order to further validate that the proposed model can effectively prevent the unit from frequently crossing the vibration zone, one of the 50 results from Algorithm A and Algorithm D is randomly selected to conduct detailed analysis and comparison. The load distribution results are shown in Figure 5.

From Figure 5, in the result from Algorithm A, all four units cross the vibration zones less number of times than seen in the result from Algorithm D, especially for unit #1. In addition, in the result from Algorithm A, unit #1 and unit #2 continue to operate with

fewer output power fluctuations. However, with Algorithm D, unit #1 shuts down after operating for approximately 9 h, and the output fluctuates greatly during the operation. With the two algorithms, units #3 and #4 have the same operating time but in terms of output power fluctuation, Algorithm A obviously outperforms Algorithm D. In general, the proposed Algorithm A can effectively reduce unit output fluctuations and reduce the number of units crossing through the vibration zone.

Three indices which include 1) the average fluctuation range, 2) power distribution skewness, and 3) fluctuation to power output ratio are proposed to quantify the result and further verify the performance of the proposed algorithm.

The average fluctuation range S_{AVR} is used to characterize the fluctuation of the unit power output in two consecutive time intervals. A larger value indicates a stronger fluctuation. The average fluctuation range can be calculated using Eq. 10:

$$S_{AVR}^i = \frac{1}{T} \sum_{t=1}^{T-1} \left(\frac{P_{i,t+1} - P_{i,t}}{P_{i,max}} \times 100\% \right). \quad (10)$$

The skewness of the power distribution S_p is an effective indicator to reflect the severity of the overall change of the power output, and its value is proportional to the severity degree. This index can be calculated as in Eq. 11:

$$S_p^i = \frac{1}{T} \sum_{t=1}^T \left(\frac{P_{i,t} - \bar{P}_i}{\sqrt{\frac{\sum_{t=1}^T (P_{i,t} - \bar{P}_i)^2}{T}}} \right)^3. \quad (11)$$

The fluctuation to power output ratio S_{\epsilonpsilon} is defined as the ratio of the average output fluctuation over the maximum power output. It can be calculated as in Eq. 12 and can characterize the fluctuation trend.

$$S_{\epsilonpsilon}^i = \frac{\sum_{t=1}^T |P_{i,t+1} - P_{i,t}|}{T \sum_{t=1}^T P_{i,t}} \times 100\%. \quad (12)$$

The values of the four indices from 50 results are averaged and compared in Table 2. From Table 2, the three indices all show that the proposed Algorithm A achieves a better performance in terms of reducing the overall power output fluctuation.

Among the three indicators, the reduction in the indicator of average fluctuation range, which evaluates the unit output change in two consecutive time intervals, is the most obvious. When compared with Algorithm D, the reduction can be as high as 81.76% with Algorithm A. Of the four units, unit #1 has the most significant reduction, as high as 88.1%. This validates the effectiveness of Algorithm A. When compared with Algorithm D, Algorithm A reduces the indicator of the fluctuation to power output ratio of the four units by 39.2%, 25.47%, 28.14%, and 42.06%, respectively, in which unit #4 has the biggest reduction. The result of Algorithm A shows a larger skewness of power distribution than does Algorithm D. This is because the power distribution skewness index evaluates the deviation of the unit power output referring to the average in each time interval. In the load distribution results of Algorithm A, the unit output is within a certain range around the average value, but the trend of change is relatively stable, while the output of Algorithm D frequently oscillates around the average value. In general, the fluctuation ranges of the power output of the four

units with Algorithm A are smaller than that with Algorithm D, which shows the superiority of Algorithm A.

5 Conclusion

This study proposes a hydropower optimal operation model that considers the risk of vibration zone crossing for cascaded hydropower plants. It can greatly reduce water consumption and effectively reduce unnecessary vibration crossing times of the units, while ensuring that their schedules satisfy the operational constraints of the hydropower plant.

The proposed two-layer intelligent optimization algorithm has a strong ability to achieve global optimization. This method can effectively suppress unit output fluctuations and operational instability caused by load fluctuations and unit commitment changes.

Data availability statement

The original contributions presented in the study are included in the article/Supplementary Material; further inquiries can be directed to the corresponding author.

Author contributions

SH and WY contributed to the conception and design of the study. LJ and LT organized the database. QH performed the statistical analysis. QH and LT wrote the first draft of the manuscript. QH, LT, SH, and WY wrote sections of the manuscript. All authors contributed to the manuscript revision, and read and approved the submitted version.

Funding

This work is projects funded by the Sichuan Science and Technology Program (No. 2023YFQ0073). The authors are grateful for the financial support.

Conflict of interest

QH, LT, LJ, and WY were employed by the company Southwest Electric Power Design Institute Co., Ltd.

The remaining author declares that the research was conducted in the absence of any commercial or financial relationships that could be construed as a potential conflict of interest.

Publisher's note

All claims expressed in this article are solely those of the authors and do not necessarily represent those of their affiliated organizations, or those of the publisher, editors, and reviewers. Any product that may be evaluated in this article, or claim that may be made by its manufacturer, is not guaranteed or endorsed by the publisher.

References

- An, Y., Fang, W., Ming, B., and Huang, Q. (2015). Theories and methodology of complementary hydro/photovoltaic operation: Applications to short-term scheduling. *J. Renew. Sustain. Energy* 7, 063133–63213. doi:10.1063/1.4939056
- Bai, K. F., Gu, J., Peng, H. Q., and Zhu, B. R. (2018). Optimal allocation for multi-energy complementary microgrid based on scenario generation of wind power and photovoltaic output. *Automation Electr. Power Syst.* 42, 133–141. doi:10.7500/aeps20170913008
- Chen, D. J., Gong, Q. W., Qiao, H., and Zhao, J. (2012). Multi-objective generation dispatching for wind power integrated system adopting improved biogeography-based optimization algorithm. *Proc. CSEE* 31, 150–158. doi:10.13334/j.0258-8013.pcsee.2012.31.015
- Cheng, C. T., Wang, J. Y., and Wu, X. Y. (2016). Hydro unit commitment with a head-sensitive reservoir and multiple vibration zones using MILP. *IEEE Trans. Power Syst.* 31, 4842–4852. doi:10.1109/TPWRS.2016.2522469
- Dong, F. F., Liu, D. C., Wu, J., Pan, X. D., Wang, H. L., Zhao, Y. J., et al. (2014). A method of constructing core backbone grid based on improved BBO optimization algorithm and survivability of power grid. *Proc. CSEE* 16, 2659–2667. doi:10.13334/j.0258-8013.pcsee.2014.16.016
- Feng, X. L., and Chou, B. Y. (2012). Optimal operation models and comparison of their energy-saving effects for large pumping station system. *Trans. Chin. Soc. Agric. Eng.* 23, 46–51. doi:10.3969/j.issn.1002-6819.2012.23.007
- Gong, Y., Cheng, J. L., Zhang, R. T., and Zhang, L. H. (2011). Decomposition dynamic programming aggregation method for optimal operation of frequency conversion and speed change of Huaiyin three stations. *Trans. Chin. Soc. Agric. Eng.* 27, 79–83. doi:10.3969/j.issn.1002-6819.2011.03.014
- Hu, L., Shen, J. J., and Tang, H. (2017). AGC control strategy of hydropower station considering complex constraints. *Proc. CSEE* 37, 5643–5654. doi:10.13334/j.0258-8013.pcsee.161758
- Jiang, Y. C., He, Z. N., and Liu, A. L. (2018). A complementary optimal operation strategy of wind power-hydropower based on improved biogeography-based optimization algorithm. *Power Syst. Prot. Control* 46, 39–47. doi:10.7667/pspc170751
- Jiang, Y. C., He, Z. N., and Liu, A. L. (2018). Wind power and hydropower complementary optimal operation strategy based on improved BBO algorithm. *Power Syst. Prot. Control* 46, 39–47. doi:10.7667/PSPC170751
- Li, J. L., Guo, B. Q., Niu, M., Xiu, X. Q., and Tian, L. T. (2018). Optimal configuration strategy of energy storage capacity in wind/PV/storage hybrid system. *Trans. China Electrotech. Soc.* 6, 1189–1196. doi:10.19595/j.cnki.1000-6753.tces.171113
- Ren, H. Y., Guo, C. X., Yang, R. F., and Wang, S. C. (2023). Fault diagnosis of electric rudder based on self-organizing differential hybrid biogeography algorithm optimized neural network. *Measurement* 208, 0263–2241. doi:10.1016/j.measurement.2022.112355
- Sun, J., Gao, Y. H., and Wang, C. (2013). Reactive power optimization based on biogeography-based optimization algorithm. *J. Nanchang Univ.* 35, 380–384. doi:10.3969/j.issn.1006-0456.2013.04.016
- Tian, D., Chen, Z. L., and Deng, Y. (2018). Operation optimization of energy storage system in wind power based on demand side response and cost model. *Trans. Chin. Soc. Agric. Eng.* 34, 200–206. doi:10.11975/j.issn.1002-6819.2018.15.025
- Xu, G., Ruan, Q. S., Tang, Z. Y., Ren, Y. F., Xu, Y., and Jiang, P. A. (2022). Study on unit commitment algorithm of Three Gorges hydropower plant based on group theory. *J. Hydroelectr. Eng.* 41, 85–94. doi:10.11660/slfdx.20220709
- Yang, X. Y., Fan, X. D., and Chen, Q. Y. (2019a). Control strategy of hydropower plant considering vibration zone and its application in wind-water coordinated operation. *Proc. CSEE* 39, 5433–5441. doi:10.13334/j.0258-8013.pcsee.190365
- Yang, Z., Yang, K., Wu, Y., Xia, Y., Qi, W. Q., Zhang, T. Y., et al. (2019b). Application of short-term hydropower generation scheduling in a hydropower station based on improved binary —real-coded shuffled frog leaping algorithm. *J. Tianjin Univ.* 52, 979–989. doi:10.11784/tdxbz201801105
- Ye, L., Qu, X. X., Yao, Y. X., Zhang, J. T., Huang, Y. H., and Wang, W. S. (2018). Analysis on intraday operation characteristics of hybrid wind-solar-hydro power generation system. *Automation Electr. Power Syst.* 42, 158–164. doi:10.7500/aeps20170915010
- Yu, Y., Wu, Y. G., and Liu, X. L. (2020). Study on daily economic load distribution strategy of hydropower station AGC based on risk control of unit crossing vibration zone. *Power Syst. Technol.* 7, 2673–2682. doi:10.13335/j.1000-3673.pst.2019.1013
- Zhang, Y. N., Zheng, X. H., Li, J. D., and Du, X. Z. (2019). Experimental study on the vibrational performance and its physical origins of a prototype reversible pump turbine in the pumped hydro energy storage power station. *Renewable Energy: An International Journal* 130, 667–676. doi:10.1016/j.renene.2018.06.057
- Zhao, B., Wang, X. J., Zhang, X. S., and Zhou, J. H. (2018). Two-layer method of microgrid optimal sizing considering demand-side response and uncertainties. *Trans. China Electrotech. Soc.* 33, 3284–3295. doi:10.19595/j.cnki.1000-6753.tces.170388
- Zhao, J., Gong, Q. W., Chen, D. J., and Liu, D. (2013). Fuzzy-dominance combined biogeography-based optimization algorithm and its application in dispatch of power system with wind farm. *Electr. Power Autom. Equip.* 3, 123–128. doi:10.3969/j.issn.1006-6047.2013.03.021
- Zhao, X., Liang, Y., Sun, M. Y., and Mao, Y. (2022). Convex relaxation and Bi-level iterative algorithm for dynamic optimal dispatch model of automatic generation control units. *Automation Electr. Power Syst.* 46, 228–238. doi:10.7500/AEPS20211012004
- Zhao, Z. P., Cheng, C. T., Liao, S. L., Li, Y. P., and Lu, Q. (2021). A MILP based framework for the hydro unit commitment considering irregular forbidden zone related constraints. *IEEE Trans. Power Syst.* 3, 1819–1832. doi:10.1109/TPWRS.2020.3028480
- Zhi, B. P., Wang, Y., Qin, J. J., Yu, Y., and Zhang, H. Z. (2019). A study on the hydropower station units' vibration based on the second-order perturbation. *J. Vib. Shock* 38, 45–49. doi:10.13465/j.cnki.jvs.2019.04.008
- Zhu, Y. M., Huang, W. B., Chen, S. J., Ma, G. W., and Han, X. Y. (2021). Intra-day Optimal Operation Strategy of Hydro-PV Hybrid System. *Advanced Engineering Sciences* 53, 142–149. doi:10.15961/j.jsuese.20200603
- Zhu, F. L., Zhong, P. A., Sun, Y. M., Xu, B., Ma, Y. F., and Liu, W. F. (2020). A coordinated optimization framework for long-term complementary operation of a large-scale hydro-photovoltaic hybrid system: Nonlinear modeling, multi-objective optimization and robust decision-making. *Energy Conversion and Management*, 226–113543. doi:10.1016/j.enconman.2020.113543